PHYSICAL REVIEW A VOLUME 18, NUMBER 3 SEPTEMBER 1978

Kinetic theory of self-diffusion in a hard-sphere fluid

Robert I. Cukier* and J. R. Mehaffey
Department of Chemistry, Michigan State University, East Lansing, Michigan 48824
(Received 24 April 1978)

A repeated-ring kinetic equation for the velocity-autocorrelation function in a hard-sphere fluid is presented. In this theory contributions from uncorrelated (Enskog) collisions, correlated (single-ring) collisions, and multiple (repeated-ring) collisions are included. A quasihydrodynamic approximation is made to describe the intermediate propagation between correlated collisions. We obtain an expression for the self-diffusion coefficient D which suggests that its density dependence arises from a competition between the shear and density fluctuations of the fluid. Using interpolation formulas to numerically evaluate the coupling of the test-particle motion to the fluid fluctuations we have computed D. The variation of D with density is found to be in good qualitative agreement with computer molecular-dynamics simulation. For low to moderate density the coupling of the test-particle motion to the fluid shear (vortex) fluctuations leads to an enhancement of D relative to its Enskog value. At high density the coupling to the fluid-density fluctuations yields a sharp decrease in D.

I. INTRODUCTION

The self-diffusion coefficient D of a monatomic hard-sphere fluid relative to the Enskog value D_E is known, from molecular dynamics simulation,[1] first to grow larger than one and then to decrease to less than one as the density increases from the dilute gas to the liquid state. The enhancement of D relative to D_E has been ascribed to the coupling of the shear modes of the fluid to the diffusing particle's motion. The reduction of D relative to D_E may be due to a molecular caging effect whereby fluctuations in the fluid density can impede the diffusing particle's motion. The competition between these two effects can then, in principal, lead to the observed behavior of D/D_E as a function of density.

In this paper, we study this self-diffusion problem by employing the repeated-ring kinetic theory of test-particle motion that we have recently derived.[2,3] This description of the thermal motion of a test particle of arbitrary size and mass was obtained by using the techniques of fully renormalized kinetic theory developed by Mazenko.[4] By systematic approximation to the exact equations of motion for the test-particle phase-space density correlation function, the dynamics were expressed in terms of the Enskog binary-collision operator. This collision operator incorporates the equilibrium correlations of the fluid. In addition to the Enskog (dynamically uncorrelated collisions), and ring (two correlated collisions) events, we incorporated repeated-ring (three, four, ... correlated collisions) events in the kinetic theory.[5] These multiply correlated recollisions play an important role in test-particle motion when the fluid mean free path l is small relative to the test-particle diameter σ since, in this limit, the test particle can collide repeatedly with a given set of neighbors.

For an arbitrary test particle, $\sigma \gg l$ can always be satisfied by choosing the particle to be sufficiently large. We first studied[2,3] this large-particle limit since here the solution of the repeated-ring kinetic equation is the simplest to effect. In particular, the coupling of test-particle motion to the fluid is dominated by the fluid transverse (shear) modes. Furthermore, the large test particle only samples the hydrodynamic behavior of the fluid motion. Thus, for a large test particle the analysis of the kinetic equation simplified considerably. We were able to show that, in this simpler situation, the contribution to the dynamics from the repeated rings could be expressed in terms of the single-ring contribution. The resulting expression for the test-particle velocity-autocorrelation function could then be resummed and led to a Stokes Einstein–like relation for the diffusion coefficient.

Even in a monatomic fluid, multiply correlated recollisions will be increasingly significant as the density increases since the fluid mean free path is considerably smaller than the particle diameter at sufficiently high density (at the highest hard-sphere density $l \approx 0.026\sigma$). Thus a repeated-ring theory is also required for a dense monatomic fluid. Moreover, there will be significant coupling of the test particle's motion to the fluid density fluctuations and other fluid modes. In particular, at high fluid density there is evidence[6] for the formation of a molecular cage whereby a test particle spends many collision times interacting with a set of nearby fluid particles. Thus, it is crucial to the description of self-diffusion to use a repeated-ring kinetic theory and include at least the coupling to fluid density fluctuations in addition to the shear mode contribution.

In Sec. II of this paper we show that the repeated-

ring contributions arising from couplings other than to the fluid shear motion can also be expressed in terms of single-ring quantities. To do so we employ the quasihydrodynamic approximation used previously to analyze single-ring theories[7] and the repeated-ring theory.[2,3] In this approximation the propagation between correlated collisions is expressed in terms of the conserved variable correlation functions with the remaining contributions approximated by a single relaxation-time term. An interesting and important asymmetry arises among the different possible fluid couplings to the test-particle motion which shows that the repeated-ring series cannot be summed in the same form as was done for solely the shear mode contributions.[2,3] Nevertheless, by suitable rearrangement, the series can be summed. If we keep the dominant couplings [cf. Eq. (2.20)] we obtain the simple and remarkably suggestive expression

$$D/D_E=(1+R_\perp)/(1-R_n)\,. \tag{1.1}$$

The quantity $R_\perp$ is a function of the coupling of the fluid shear motion to the test-particle motion and R_n plays the same role for the fluid density fluctuations. We shall show the $R_\perp$ is a positive increasing function of density while R_n is a negative decreasing function of density. Thus, in principal, D/D_E can exhibit the known variation with density.

For a molecular test particle the coupling to the fluid motion as in $R_\perp$ and R_n is not solely controlled by hydrodynamics. The proper short-time and small-distance behavior must also be incorporated as well as the nonconserved variable contributions. This substantially complicates the analysis. In Sec. III we use formulas devised by Résibois[8] and Furtado *et al.*[7] to approximate the conserved variable correlation functions required to evaluate $R_\perp$ and R_n. These expressions are used to evaluate D/D_E and the results compared with the molecular-dynamics simulation.[1] In Sec. IV we summarize our results and discuss the approximations that they rely upon.

II. REPEATED-RING KINETIC THEORY

In the repeated-ring kinetic theory,[2,3] the Laplace transform of the test-particle velocity-autocorrelation function

$$\psi_v(z)=-i\int_0^\infty dt\, e^{izt}\langle\vec{v}(t)\cdot\vec{v}(0)\rangle_0 \tag{2.1}$$

satisfies the kinetic equation

$$[z-\Lambda(z)-R(z)]\psi_v(z)=\langle v^2(0)\rangle_0\,. \tag{2.2}$$

In Eqs. (2.1) and (2.2) $\vec{v}(t)$ is the test-particle velocity at time t. The quantities Λ and R in Eq. (2.2) are the Enskog and repeated-ring memory functions, respectively.

For a fluid of hard spheres, the Enskog memory function, which incorporates the contributions to the dynamics from uncorrelated collisions, is frequency independent. It is

$$\Lambda(z)=-i\lambda_E=-i\tfrac{2}{3}\tau_E^{-1}\,, \tag{2.3}$$

where the Enskog collision frequency[9] is

$$\tau_E^{-1}=4ng(\sigma)\sigma^2(\pi k_BT/m)^{1/2}\,. \tag{2.4}$$

In Eq. (2.4), n is the fluid number density, T is the temperature, σ is the hard-sphere diameter, m is the mass of a particle, $g(\sigma)$ is the radial distribution function at contact, and k_B is Boltzmann's constant.

The repeated-ring memory function $R(z)$ contains the contributions to the dynamics from multiply correlated collisions. It can be written in the form[2,3]

$$\begin{aligned}R(z)=-n^{-1}\mathcal{V}^{-1}\int d1\,d2\,(mk_BT)^{-1/2}p_{1z}\tau(1;3\bar{3})\\ \times[G_D(3\bar{3};4\bar{4})+G_D(3\bar{3};5\bar{5})T(5\bar{5};6\bar{6})G_D(6\bar{6};4\bar{4})+G_D(3\bar{3};5\bar{5})T(5\bar{5};6\bar{6})G_D(6\bar{6};7\bar{7})\\ \times T(7\bar{7};8\bar{8})G_D(8\bar{8};4\bar{4})+\cdots]\tau^T(4\bar{4};2)(mk_BT)^{-1/2}p_{2z}\,.\end{aligned} \tag{2.5}$$

In Eq. (2.5), $\mathcal{V}$ is the volume of the system. The notation $1\equiv(\vec{r}_1,\vec{p}_1)$ denotes the field point phases and p_{1z} the laboratory z component of the momentum $\vec{p}_1$. We use the notation that unbarred integers $(1,2,\ldots)$ represent the field points associated with the test particle while barred integers $(\bar{1},\bar{2},\ldots)$ represent the field points associated with bath particles. Note that in Eq. (2.5), integration over repeated field points is implied. The operators τ, T, and τ^T represent binary collisions between the test particle and bath particles. They can be expressed in terms of the hard-sphere Enskog collision operator[10] $T_E(3\bar{3})$, where

$$\begin{aligned}T_E(3\bar{3})=ig(\sigma)\left(\frac{\vec{p}_{\bar{3}3}\cdot\hat{r}_{\bar{3}3}}{m}\right)\theta(\vec{p}_{\bar{3}3}\cdot\hat{r}_{\bar{3}3})\\ \times\delta(|\vec{r}_{\bar{3}3}|-\sigma)[b_{\bar{3}3}-1]\,.\end{aligned} \tag{2.6a}$$

In Eq. (2.6a) the unit vector joining the centers of the spheres at contact is $\hat{r}_{\bar{3}3}=(\vec{r}_{\bar{3}}-\vec{r}_3)/\sigma=\vec{r}_{\bar{3}3}/\sigma$, the precollision relative momentum is $\vec{p}_{\bar{3}3}=\vec{p}_{\bar{3}}-\vec{p}_3$, and the heaviside step function is $\theta(x)=1$ for

$x \geq 0$ and $\theta(x) = 0$ for $x < 0$. The operator $b_{\bar{3}3}$ changes the precollision momenta of the two particles to their postcollision values; i.e., $b_{\bar{3}3} f(\vec{p}_3, \vec{p}_{\bar{3}}) = f(\vec{p}_3^*, \vec{p}_{\bar{3}}^*)$ where

$$\vec{p}_3^* = \vec{p}_3 + \hat{r}_{\bar{3}3}(\hat{r}_{\bar{3}3} \cdot \vec{p}_{\bar{3}3})$$

and

$$\vec{p}_{\bar{3}}^* = \vec{p}_{\bar{3}} - \hat{r}_{\bar{3}3}(\hat{r}_{\bar{3}3} \cdot \vec{p}_{\bar{3}3}) . \tag{2.6b}$$

The propagator G_D in Eq. (2.5) is

$$G_D(3\bar{3}; 4\bar{4}) = -i \int_0^\infty dt\, e^{izt} C_{s_E}(34, t) C_E(\bar{3}\bar{4}, t) , \tag{2.7}$$

where C_{s_E} is the phase-space test-particle correlation function and C_E the phase-space density correlation function, both evaluated in the Enskog approximation.

The interpretation of $R(z)$ is straightforward. Initially the test particle with momentum $\vec{p}_2$ undergoes a collision $[\tau^T(4\bar{4}; 2)]$ with a typical bath particle selected from a Boltzmann distribution of particles. The postcollision coordinates of the test particle and its collision partner are $4 = (\vec{r}_4, \vec{p}_4)$ and $\bar{4} = (\vec{r}_{\bar{4}}, \vec{p}_{\bar{4}})$, respectively. Each term in the square brackets of Eq. (2.5) represents contributions from different dynamical processes which can now occur. The first term (the ring term) represents the process in which the test particle and its collision partner undergo Enskog propagation but independently of one another $[G_D(3\bar{3}; 4\bar{4})]$. The initial correlation is communicated to the test particle when it undergoes a collision $[\tau(1; 3\bar{3})]$ with its initial collision partner (or one dynamically related to it) at the precollision field point 3 and $\bar{3}$, respectively. The test particle then recoils with momentum $\vec{p}_1$. The second term (the first repeated-ring term) in the square brackets of Eq. (2.5) represents the process in which, following the initial collision $[\tau^T(4\bar{4}; 2)]$, the intermediate propagation $[G_D(5\bar{5}; 4\bar{4})]$ leads to a collision $[T(6\bar{6}; 5\bar{5})]$ at $5, \bar{5}$ in which the test particle and bath particle recoil with field points 6 and $\bar{6}$, respectively. The two particles now undergo independent Enskog propagation $[G_D(3\bar{3}; 6\bar{6})]$ until the final collision at $3, \bar{3}$ $[\tau(1; 3\bar{3})]$ where the test particle recoils with momentum $\vec{p}_1$. In this fashion, by treating each of the terms in Eq. (2.5) in succession, one includes the contribution to the test-particle velocity-autocorrelation function from processes in which the test particle undergoes any number of correlated collisions with a bath particle. Note that the intermediate field points, $4\bar{4}, 5\bar{5}$, etc., are all averaged (integrated) over and in the final step the initial and final momenta, $\vec{p}_2$ an $\vec{p}_1$, respectively, are also averaged over.[11]

The full momentum dependence in the correlation functions G_D, as well as in the collision terms τ, τ^T, and T, leads to some difficulty in the evaluation of $R(z)$. The techniques employed to approximate the intermediate propagation G_D in the repeated-ring memory function $R(z)$ were presented elsewhere in detail[3] and will simply be sketched here. First one introduces the spatial Fourier transform of the correlation functions G_D; this introduces intermediate wave vectors $\vec{q}, \vec{q}', \ldots$. The laboratory z components of $\vec{p}_1$ and $\vec{p}_2$ are expressed in the appropriate wave-vector reference frame. The momentum dependent correlation functions $C_{s_E}(\vec{q}, \vec{p}_3, \vec{p}_4; t)$ and $C_E(-\vec{q}, \vec{p}_{\bar{3}}, \vec{p}_{\bar{4}}; t)$ are then expanded in a complete momentum representation. The first five basis functions are $H_1^q(\vec{p}) = 1$, $H_2^q(\vec{p}) = \xi_{x_q}$, $H_3^q(\vec{p}) = \xi_{y_q}$, $H_4^q(\vec{p}) = \xi_{z_q}$, and $H_5^q(\vec{p}) = \frac{1}{6}(\xi^2 - 3)$ where $\xi_{z_q} = (mk_BT)^{1/2} p_{z_q}$ is the z component of the dimensionless momentum in the $\vec{q}$ reference frame.[12] Finally one makes the quasihydrodynamic approximation[7] to the product of $C_{s_E}(\vec{q}, \vec{p}_3, \vec{p}_4; t)$ and $C_E(-\vec{q}, \vec{p}_{\bar{3}}, \vec{p}_{\bar{4}}; t)$. In this approximation the projections onto the conserved variable momentum states are treated exactly while the projections onto the nonconserved variables are approximated in a simple manner, [cf. Eq. (2.11)]. In the quasihydrodynamic approximation, the repeated-ring memory function is

$$\begin{aligned} R(z) = n \sum_{K,M=2}^{4} \sum_{I,J=1}^{5} \left(\frac{1}{2\pi}\right)^3 \int d\vec{q}\, \epsilon_K B_{KI}(q) \Delta_{IJ}(q, z) \epsilon_M B_{MJ}(q) \\ + n \sum_{K=2}^{4} \sum_{I,J=1}^{5} \left(\frac{1}{2\pi}\right)^3 \int d\vec{q}\, n \sum_{K'=2}^{4} \sum_{I',J'=1}^{5} \left(\frac{1}{2\pi}\right)^3 \int d\vec{q}'\, \epsilon_K B_{KI}(q) \Delta_{IJ}(q, z) \\ \times \Big(T_{JI'}(\vec{q} + \vec{q}') + n \sum_{I'',J''=1}^{5} \left(\frac{1}{2\pi}\right)^3 \int d\vec{q}''\, T_{JI''}(\vec{q} + \vec{q}'') \Delta_{I''J''}(q'', z) \\ \times T_{J''I'}(\vec{q}'' - \vec{q}') + \cdots \Big) \Delta_{I'J'}(q', z) B_{K'J'}(q') \epsilon_{K'} . \end{aligned} \tag{2.8}$$

TABLE I. Factors $B_{KI}(q)$.[a]

KI	$B_{KI}(q)$
22=33	$4i\,j_1(q\sigma)/q\sigma$
44	$4i[j_0(q\sigma)-2j_1(q\sigma)/q\sigma]$
41	$4\sqrt{\pi}\,j_1(q\sigma)$
45	$(\frac{1}{6}\pi)^{1/2}j_1(q\sigma)$

[a] Factors $B_{KI}(q)$ are listed here in units of $(2n\tau_E)^{-1}$. The function j_k is the spherical Bessel function of order k.

In Eq. (2.8), the summations over K, M, and K' as well as the factors ϵ_K, ϵ_M, and $\epsilon_{K'}$ arise from expressing the laboratory z components of $\vec{p}_1$ and $\vec{p}_2$ in the $\vec{q}$ (or $\vec{q}'$) reference frame. Note that $\epsilon_2 = \sin\theta_q\cos\phi_q$, $\epsilon_3 = \sin\theta_q\sin\phi_q$, and $\epsilon_4 = \cos\theta_q$ where θ_q, ϕ_q, and ψ_q are the Euler angles[13] of the $\vec{q}$ reference frame relative to the laboratory reference frame. The $B_{KI}(q)$ factors are matrix elements of the hard-sphere Enskog collision operator,

$$B_{KI}(q)=\int d\vec{r}_{\bar{4}4}\int d\vec{p}_4\,d\vec{p}_{\bar{4}}\,e^{-i\vec{q}\cdot\vec{r}_{\bar{4}4}}f_0(p_4)f_0(p_{\bar{4}}) \times H_I^q(\vec{p}_{\bar{4}})T_E(4\bar{4})H_K^q(\vec{p}_4)\,, \tag{2.9}$$

where $f_0(p_4)$ is the Maxwellian momentum distribution function. Due to the simple structure of T_E, these matrix elements can be evaluated[14] and those that are nonzero are listed in Table I. The $T_{JI'}$ factors are also matrix elements of the hard-sphere Enskog collision operator

$$T_{JI'}(\vec{q}+\vec{q}')=(n\Omega)^{-1}\int d4\,d\bar{4}\,e^{i(\vec{q}+\vec{q}')\cdot\vec{r}_{\bar{4}4}} \times f_0(p_4)f_0(p_{\bar{4}})H_J^q(\vec{p}_{\bar{4}})T_E(4\bar{4})H_{I'}^{q'}(\vec{p}_{\bar{4}})\,. \tag{2.10}$$

Following the techniques used to calculate the $B_{KI}(q)$ factors, the $T_{JI'}(\vec{q}\pm\vec{q}')$ factors are found to be given by spherical Bessel functions with argument $|\vec{q}\pm\vec{q}'|$. The quantities $\Delta_{IJ}(q,z)$, which describe the intermediate propagation between correlated collisions, are

$$\Delta_{IJ}(q,z)=-i\int_0^\infty dt\,e^{izt} \times[C_{s_{E_{11}}}(q,t)C_{E_{IJ}}(-q,t) - e^{-(\lambda_s+\lambda)t}C_{s_{0_{11}}}(q,t)C_{0_{IJ}}(-q,t)]\,, \tag{2.11}$$

where the momentum contracted correlation functions are

$$C_{E_{IJ}}(-q,t)=n^{-1}\int d\vec{p}_{\bar{3}}\,d\vec{p}_{\bar{4}}\,H_I^q(\vec{p}_{\bar{3}}) \times C_E(-\vec{q},\vec{p}_{\bar{3}},\vec{p}_{\bar{4}};t)H_J^q(\vec{p}_{\bar{4}})\,. \tag{2.12}$$

Hence $C_{s_{E_{11}}}$ and $C_{s_{0_{11}}}$ are the self parts of the van Hove correlation function in the Enskog and free-particle limits, respectively. Similarly, $C_{E_{11}}$ is the density correlation function, $C_{E_{22}}$ is the transverse current correlation function, $C_{E_{44}}$ is the longitudinal current correlation function, etc. The quantities λ_s and λ are nonconserved variable relaxation times for the single-particle and bath fluctuations, respectively. The form of Eq. (2.11) is a consequence of the quasihydrodynamic approximation for the intermediate propagation.

The wave-vector integrations $\int d\vec{q}\int d\vec{q}'\cdots$ in Eq. (2.8) for the repeated-ring memory function appear difficult due to the coupling introduced by the matrix elements $T_{JI'}(\vec{q}+\vec{q}')$. Noting that these matrix elements are proportional to spherical Bessel functions of argument $|\vec{q}+\vec{q}'|$, we utilize "addition theorems"[15] to decouple the wave-vector integrations. We have previously demonstrated how this decoupling procedure is carried out for the contribution from the transverse momentum fluctuations in the bath. In Appendix A we demonstrate that this procedure also allows us to decouple the wave-vector integrations from contributions coming from the bath density and longitudinal current fluctuations, contributions which are important in the self-diffusion process. The central result is

$$\begin{aligned}
&\int d\vec{q}_1\,d\vec{q}_2\cdots d\vec{q}_n\,\epsilon_{K_1}B_{K_1I_1}(q_1)\Delta_{I_1J_1}(q_1,z)T_{J_1I_2}(\vec{q}_1+\vec{q}_2)\Delta_{I_2J_2}(q_2,z)T_{J_2I_3}(\vec{q}_2+\vec{q}_3)\cdots\\
&\times T_{J_{n-2}I_{n-1}}(\vec{q}_{n-2}+\vec{q}_{n-1})\Delta_{I_{n-1}J_{n-1}}(q_{n-1},z)T_{J_{n-1}I_n}(\vec{q}_{n-1}-\vec{q}_n)\Delta_{I_nJ_n}(q_n,z)B_{K_nJ_n}(q_n)\epsilon_{K_n}\\
&=\int d\vec{q}_1\,\epsilon_{K_1}\epsilon_{K_1}B_{K_1I_1}(q_1)\Delta_{I_1J_1}(q_1,z)B_{K_1J_1}(q_1)(-i\lambda_E)^{-1}\\
&\times\int d\vec{q}_2\,\epsilon_{I_2}\epsilon_{J_2}B_{I_2I_2}(q_2)\Delta_{I_2J_2}(q_2,z)B_{J_2J_2}(q_2)(-i\lambda_E)^{-1}\cdots\\
&\times\int d\vec{q}_{n-1}\,\epsilon_{I_{n-1}}\epsilon_{J_{n-1}}B_{I_{n-1}I_{n-1}}(q_{n-1})\Delta_{I_{n-1}J_{n-1}}(q_{n-1},z)B_{J_{n-1}J_{n-1}}(q_{n-1})(-i\lambda_E)^{-1}\\
&\times\int d\vec{q}_n\,\epsilon_{I_n}\epsilon_{K_n}B_{I_nK_n}(q_n)\Delta_{I_nJ_n}(q_n,z)B_{K_nJ_n}(q_n)\,.
\end{aligned} \tag{2.13}$$

This equality shows that Eq. (2.8) can be written in terms of single-ring quantities. To this end we introduce the coupling of the test particle's motion in the ring approximation [first term in Eq. (2.8)] to the fluid transverse current correlations as

$$R_{\perp}^{1}(z)=2n\left(\frac{1}{2\pi}\right)^{3}\int d\vec{q}\,\epsilon_{2}B_{22}(q)\Delta_{22}(q,z)\epsilon_{2}B_{22}(q)\,, \tag{2.14a}$$

to the fluid longitudinal current correlations as

$$R_{\parallel}^{1}(z)=n\left(\frac{1}{2\pi}\right)^{3}\int d\vec{q}\,\epsilon_{4}B_{44}(q)\Delta_{44}(q,z)\epsilon_{4}B_{44}(q)\,, \tag{2.14b}$$

and to the fluid density correlations as

$$R_{n}^{1}(z)=n\left(\frac{1}{2\pi}\right)^{3}\int d\vec{q}\,\epsilon_{4}B_{41}(q)\Delta_{11}(q,z)\epsilon_{4}B_{41}(q)\,. \tag{2.14c}$$

The factor of 2 in Eq. (2.14a) reflects the equivalence of the transverse current correlation functions $\Delta_{22}=\Delta_{33}$.

Implementing the wave-vector decoupling scheme summarized in Eq. (2.13) and utilizing the definitions (2.14), the repeated-ring memory function given by Eq. (2.8) becomes[16]

$$\begin{aligned}R(z)=&\,[R_{\perp}^{1}(z)+R_{\parallel}^{1}(z)+R_{n}^{1}(z)]\\&+[R_{\perp}^{1}(z)+R_{\parallel}^{1}(z)+R_{n}^{1}(z)](-i\lambda_{E})^{-1}[R_{\perp}^{1}(z)+R_{\parallel}^{1}(z)]\\&+[R_{\perp}^{1}(z)+R_{\parallel}^{1}(z)+R_{n}^{1}(z)](-i\lambda_{E})^{-1}[R_{\perp}^{1}(z)+R_{\parallel}^{1}(z)]\\&\times(-i\lambda_{E})^{-1}[R_{\perp}^{1}(z)+R_{\parallel}^{1}(z)]+\cdots\,.\end{aligned} \tag{2.15}$$

Note that contributions from the fluid transverse and longitudinal current correlations, $R_{\perp}^{1}(z)$ and $R_{\parallel}^{1}(z)$, appear in a symmetric manner whereas the contributions from the density correlations in the fluid, $R_{n}^{1}(z)$, appear in an asymmetric manner. Adding the Enskog and repeated-ring memory functions and summing the resulting series yields

$$\begin{aligned}\Lambda(z)+R(z)&=-i\lambda_{E}[1+R_{n}^{1}(z)/(-i\lambda_{E})]\\&\quad\times\{1+[R_{\perp}^{1}(z)+R_{\parallel}^{1}(z)]/(-i\lambda_{E})\\&\qquad+[R_{\perp}^{1}(z)+R_{\parallel}^{1}(z)]^{2}/(-i\lambda_{E})^{2}+\cdots\}\\&=-i\lambda_{E}[1-R_{n}^{1}(z)/i\lambda_{E}]\{1+[R_{\perp}^{1}(z)+R_{\parallel}^{1}(z)]/i\lambda_{E}\}^{-1}\,.\end{aligned} \tag{2.16}$$

Substituting Eq. (2.16) into Eq. (2.2) we find that the test-particle velocity autocorrelation function is

$$\psi_{v}(z)=\left[z+i\lambda_{E}\left(1-\frac{R_{n}^{1}(z)}{i\lambda_{E}}\right)\left(1+\frac{R_{\perp}^{1}(z)+R_{\parallel}^{1}(z)}{i\lambda_{E}}\right)^{-1}\right]^{-1}\times\langle v^{2}(0)\rangle\,. \tag{2.17}$$

To compute the full time dependence of the velocity autocorrelation from Eq. (2.17) is a formidable task. First, one must calculate the ring contributions $R_{\perp}^{1}(z)$, $R_{\parallel}^{1}(z)$, and $R_{n}^{1}(z)$. To do so one must compute the various correlation functions $C_{E_{11}}(-q,t)$, $C_{E_{22}}(-q,t)$, etc., which appear in Eqs. (2.14) and then perform the time and wave-vector integrations numerically. Finally, the results for the ring contributions are to be substituted into Eq. (2.17) for $\psi_{v}(z)$ and the Laplace transform numerically inverted to obtain the full time dependence of $\psi_{v}(t)$. As a first test of our repeated-ring kinetic theory description of self-diffusion, we choose not to perform these lengthy procedures required to compute $\psi_{v}(t)$ from (2.17), but instead focus on two more readily accessible quantities: the long time behavior of $\psi_{v}(t)$, and the self-diffusion coefficient.

As is well known[17,18] the long time behavior of $\psi_{v}(t)$ is dominated by the coupling of the test-particle's motion to the fluid transverse fluctuations $R_{\perp}^{1}(z)$. For long times $R_{\perp}^{1}(z)$ is determined by the hydrodynamic (long-time) forms of the correlation functions $C_{s_{E_{11}}}(q,t)$ and $C_{E_{22}}(-q,t)$. These are $e^{-q^{2}D_{E}t}$ and $e^{-q^{2}\nu_{E}t}$, respectively, where D_{E} is the Enskog self-diffusion coefficient [cf. Eq. (2.21)] and ν_{E} is the Enskog kinematic viscosity. One finds

$$\lim_{t\to\infty}\psi_{v}(t)\sim\tfrac{2}{3}(k_{B}T/mn)[4\pi(D_{E}+\nu_{E})t]^{-3/2}\,, \tag{2.18}$$

as predicted via other kinetic theories.[18]

The self-diffusion coefficient can be expressed in terms of $\psi_{v}(z)$ as

$$D=\lim_{z\to i0^{+}}i\psi_{v}(z)\,. \tag{2.19}$$

Taking this limit in Eq. (2.17) yields

$$D=D_{E}\frac{1+[R_{\perp}^{1}(i0^{+})+R_{\parallel}^{1}(i0^{+})]/i\lambda_{E}}{1-R_{n}^{1}(i0^{+})/i\lambda_{E}}\,, \tag{2.20}$$

where the Enskog diffusion coefficient is

$$D_{E}=\langle v_{0}^{2}(0)\rangle_{0}/\lambda_{E}\,. \tag{2.21}$$

The expression (2.20) for the self-diffusion coefficient is a central result of our analysis. The numerator is a positive increasing function of density since the transverse mode coupling, which dominates the longitudinal current coupling, is inherently positive. It is this term that leads to enhancement of the self-diffusion coefficient relative to D_{E} at moderate densities. The denominator is also inherently positive since the coupling to the fluid density fluctuations, R_{n}^{1}, is negative. As

density increases the denominator grows more rapidly than the numerator and ultimately leads to the reduction of D relative to D_E at high fluid density. Thus, this competition between the shear (vortex) motion and density fluctuations (a molecular cage effect) is seen to be responsible for the self-diffusion coefficient's dependence on density.

This qualitative discussion can be made quantitative if expressions for the single ring memory functions appearing in Eq. (2.20) are available. In Sec. III, simple analytic forms for the correlation functions, $C_{s_{E_{11}}}(q,t)$ and $C_{E_{IJ}}(-q,t)$, proposed previously by Résibois[8] and Furtado *et al.*[7], are used to compute $R^1_\perp(i0^+)$, $R^1_\parallel(i0^+)$, etc. over a wide range of densities. The predicted values of the self-diffusion coefficient using Eq. (2.20) are then compared to the results of the computer molecular dynamics simulation of Alder *et al.*[1]

III. NUMERICAL RESULTS

To determine D/D_E we must evaluate the single-ring quantities $R^1_\perp(i0^+)$, $R^1_\parallel(i0^+)$, and $R^1_n(i0^+)$ given in Eqs. (2.14). These are expressed in terms of the $\Delta_{IJ}(q,z)$, defined in Eq. (2.11), which describe the propagation of test and fluid particles between the correlated collisions. We follow the techniques used by Résibois[8] and Furtado *et al.*[7] to approximate the Enskog correlation functions appearing in Eqs. (2.11) by expressions which interpolate between the correct short- and long-time forms. The short-time form is obtained from sum rules while the long-time form is obtained from generalized hydrodynamics. The nonconserved variable relaxation frequencies λ_s and λ which appear in the second term of the $\Delta_{IJ}(q,z)$ expression given in Eq. (2.11), are expressed in terms of the Enskog self-diffusion coefficient and the Enskog kinematic viscosity, respectively. The formulas required for the evaluation of the $\Delta_{IJ}(q,t)$ are collected in Appendix B. The resultant forms can be analytically Laplace transformed to yield the $\Delta_{IJ}(q,z)$. These expressions for the $\Delta_{IJ}(q,z)$ are used in Eqs. (2.14) and, with the explicit forms for the $B_{IJ}(q)$ factors given in Table I, the wave-vector integrations are performed numerically.

The resulting expressions for $R^1_\perp$, $R^1_\parallel$, and R^1_n are presented in Fig. 1 for a wide range of fluid density. We have used the density unit V/V_0, the ratio of the volume of the fluid to its volume at closest packing, to conform with the molecular-dynamics data presentation. For low and intermediate fluid densities, $V/V_0 \geq 3$, the coupling of the test particle's motion to the fluid is dominated by the transverse (vortex) modes ($R^1_\perp/i\lambda_E$). For very high fluid densities $1.5 \leq V/V_0 \leq 3$, the coupling of the test particle's motion to the fluid density fluctuations ($R^1_n/i\lambda_E$) becomes significant and increases dramatically with increasing density. Note that throughout the density range investigated, the coupling to the longitudinal fluid current fluctuations ($R^1_\parallel/i\lambda_E$) is small.

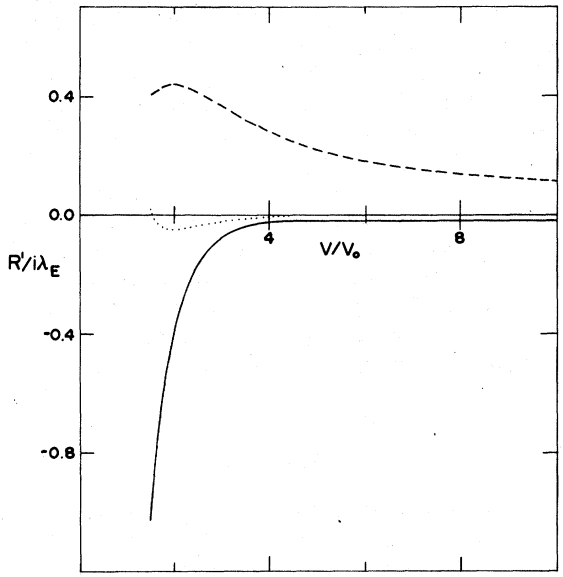

FIG. 1. Variation of the single-ring quantities with density. The solid curve is $R^1_n(i0^+)/i\lambda_E$, the dashed curve is $R^1_\perp(i0^+)/i\lambda_E$, and the dotted curve is $R^1_\parallel(i0^+)/i\lambda_E$. V/V_0 is the ratio of the volume of the fluid to its volume at closest packing.

The numerical values of $R^1_\perp$, $R^1_\parallel$, and R^1_n are substituted into Eq. (2.20) to determine the ratio D/D_E. A comparison of our calculations with the simulation of Alder *et al.* is presented in Fig. 2.

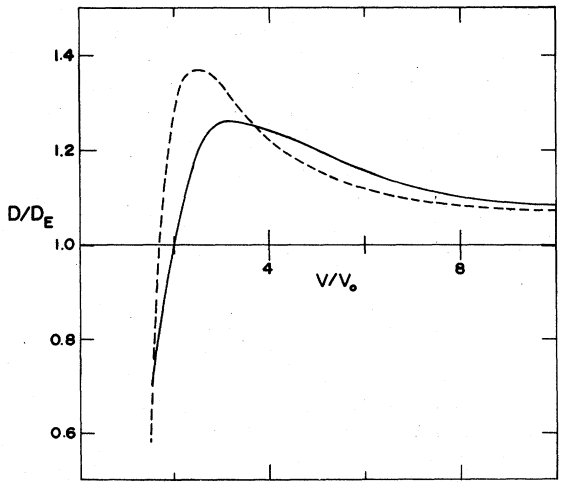

FIG. 2. The variation of the self-diffusion ratio D/D_E with density in a hard-sphere fluid. The solid curve is our result and the dashed curve is the computer molecular dynamics result of Ref. 1.

The overall agreement is encouraging. As was inferred from Eq. (2.20), the dependence of D/D_E on density arises from the competition between the coupling of the test particle's motion to the fluid transverse modes which enhance D/D_E, and the coupling to the fluid density fluctuations (the cage effect) which reduces D/D_E. The quantitative resolution of this competition, which relies on the numerical work presented in this section, shows that the inclusion of multiple recollisions and the coupling of the test particle's motion to both the shear and density fluctuations of the fluid are crucial to the description of self-diffusion at high density.

IV. DISCUSSION

We have presented an analysis of the velocity-autocorrelation function in a hard-sphere fluid in which the effects of multiply correlated collisions have been included. These multiple recollisions are increasingly important as the fluid density increases and, as shown herein, must be incorporated in a theory of self-motion in dense fluids. To simplify the Enskog propagation between correlated collisions we used the quasihydrodynamic approximation whereby the conserved variable fluctuations are treated exactly and the nonconserved variable fluctuations are expressed in terms of a single relaxation time approximation. Our central results are the expressions for the velocity-autocorrelation function and self-diffusion coefficient of Eqs. (2.17) and (2.20), respectively. With the use of interpolation formulas to describe the conserved variable correlation functions, the self-diffusion coefficient was computed as a function of fluid density. As presented in Fig. 2, our calculation of the self-diffusion coefficient exhibits the essential behavior seen in the molecular dynamics simulation.

What can account for the lack of agreement between the simulation and our numerical results? There are several approximations that may lead to this lack of precise agreement: those employed in the derivation of the kinetic equation itself, the quasihydrodynamic approximation, the modeling of the resultant correlation functions describing the intermediate propagation, and the choice of the relaxation frequencies λ_s and λ.

The kinetic equation, Eq. (2.2), previously derived[2,3] and analyzed here for self-diffusion is an approximation to a many-body problem. Where rigorous results are available, our kinetic theory will reproduce them, but once away from the Boltzmann-Enskog regime or the asymptotic time regime at low density, the only test of the theory is comparison with experiment or simulation. Unfortunately, this test of the kinetic theory also relies on further approximations which must be made to solve the kinetic equation.

To describe the intermediate propagation between correlated collisions, the quasihydrodynamic approximation is used [cf. Eq. (2.8)]. In this scheme the momentum dependence of the Enskog phase-space correlation functions is expanded in a momentum basis. The projections onto conserved variables are then exactly accounted for while the remaining momentum dependence is approximated via a single relaxation-time term. Further improvements here may require the use of a better basis set involving the wave-vector-dependent eigenfunctions of the Enskog propagator.

The conserved variable correlation functions appearing in Eq. (2.11) are approximated by the interpolation formulas presented in Appendix B. They will be accurate, by construction, at short and long times. For the transition regime, it is hoped that they provide an adequate description of the conserved variable correlation functions. More-accurate correlation functions could be constructed through the use of kinetic modeling[19] at the expense of a greater computational effort. The choice of the single relaxation frequencies λ_s and λ in Eq. (2.11) is another approximation. We have repeated our calculations using $\lambda = \frac{4}{5}$ rather than $\lambda = 1/\tilde{\nu}_E$ (cf. Appendix B) and found the variation of D/D_E with respect to density remains the same. The computed values are, however, slightly reduced in the density range $2 < V/V_0 < 5$ relative to those using $\lambda = 1/\tilde{\nu}_E$; the low- and high-density results are insensitive to the choice of λ. By contrast, the single-ring quantities $R_\perp^1$, $R_\parallel^1$, and R_n^1 are somewhat dependent on the choice of λ and this leads to a *single*-ring theory for D/D_E which reflects this dependence.

To summarize, a more extensive basis set along with a more accurate evaluation of the resulting expansion coefficients may well lead to better agreement with the molecular-dynamics simulation data. However, to go beyond the procedures adopted here, a much larger numerical effort will be required.

In our theory the correlated collisions between test and fluid particles are expressed in terms of the Enskog binary collision operator and the intermediate propagation between these correlated collisions in terms of Enskog propagators. Thus, what is required as input here are the properties of the Enskog fluid. This is an exceedingly useful result in that the Enskog fluid, where there are no dynamical correlations, is much easier to describe theoretically than is the actual fluid.

Throughout this work we have stressed that to treat a dense fluid properly, multiply correlated

collisions must be incorporated in the theory. For a large test particle, the intermediate propagation between correlated collisions is dominated by the coupling to the shear motion of the fluid. This leads to a diffusion coefficient of the Stokes-Einstein form.[2,3] In a monatomic fluid, the coupling to the fluid density fluctuations also becomes crucial. The numerical results (cf. Fig. 2) show that the effect of these density fluctuations grows dramatically at high density. This is in accord with the physical conception of a molecular cage. Hence, we feel that the kinetic theory expression of a molecular cage effect is realized through a repeated-ring theory including the coupling to the fluid density fluctuations.

In this and preceding papers we have considered the large-test-particle limit and the monatomic fluid. The treatment of the thermal fluctuations of a test particle of arbitrary size and mass can be carried out in the same spirit as presented here. The contributions to D/D_E arising from the density, shear, and other fluctuations will be modulated by the mass- and size-dependent B factors as well as the different motional time scale of the test-particle intermediate propagator. Thus, we anticipate that the interesting phenomena that have been elucidated by molecular-dynamics simulations[6,20] on test particles of differing size and mass can be interpreted within the general formalism that we have developed.

ACKNOWLEDGMENTS

This work was supported in part by grants from NSF. One of us (R.I.C.) was supported in part by a fellowship from the Alfred P. Sloan Foundation.

APPENDIX A

In this Appendix we investigate the angular integrations over the matrix elements $T_{JI'}(\vec{q}+\vec{q}')$ which appears in Eq. (2.8). Following techniques analogous to those employed to calculate the matrix elements[14] B_{MJ} one finds that

$$T_{JI'}(\vec{q}+\vec{q}') = -(i/2\pi)(n^2\tau_E)^{-1}K_{JI'}(\vec{q}+\vec{q}') , \tag{A1}$$

where

$$K_{JI'}(\vec{q}+\vec{q}') = \begin{cases} 0 & \text{if } I'=1 \\ \int d\hat{\rho}\, H_J^q(\hat{\rho})H_{I'}^{q'}(\hat{\rho})e^{-i(\vec{y}+\vec{y}')\cdot\hat{\rho}}, & \text{if } J,I'=2,3,4 \\ \frac{\sqrt{\pi}}{2}\int d\hat{\rho}\, H_{I'}^{q'}(\hat{\rho})e^{-i(\vec{y}+\vec{y}')\cdot\hat{\rho}}, & \text{if } J=1 . \end{cases} \tag{A2}$$

In Eq. (A2), $\vec{y}\equiv\vec{q}\sigma$, $\vec{y}'\equiv\vec{q}'\sigma$, and $\hat{\rho}$ is a unit vector. Note also that we have not included the coupling to the energy states $J=5$ or $I'=5$. From Eq. (2.8), it is clear that in the first repeated-ring contribution [that is, the second term in Eq. (2.8)] we must evaluate angular integrals of the form

$$\kappa_{KJI'K'}(\vec{q}+\vec{q}') = \int d\hat{\Omega}_q \int d\hat{\Omega}_{q'} \epsilon_K T_{JI'}(\vec{q}+\vec{q}')\epsilon_{K'} , \tag{A3}$$

where

$$\int d\hat{\Omega}_q \cdots = \frac{1}{2\pi}\int_0^{2\pi} d\psi_q \int_0^{2\pi} d\phi_q \int_0^{\pi} d\theta_q \sin\theta_q \cdots \tag{A4}$$

is an integration over the Euler angles. There are twelve nonzero $\kappa_{KJI'K'}$ factors and, due to the rotational symmetry of the fluid, some of them are interrelated. They are $\kappa_{2222}=\kappa_{2233}=\kappa_{3322}=\kappa_{3333}$; $\kappa_{2244}=\kappa_{3344}$; $\kappa_{4422}=\kappa_{4433}$; κ_{4444}; $\kappa_{4122}=\kappa_{4133}$; and κ_{4144}.

In Appendix C of Ref. 1 we have demonstrated that for the coupling to the transverse current fluctuations

$$\kappa_{2222}(\vec{q}+\vec{q}') = (\tfrac{4}{3}\pi)^2 B_{22}(q)(-i\lambda_E)^{-1}B_{22}(q') . \tag{A5}$$

Let us now turn our attention to κ_{4444}. Since $H_4^q(\hat{\rho}) = \rho_{z_q} = \hat{\rho}\cdot\vec{y}/y$, we can write

$$K_{44}(\vec{q}+\vec{q}') = -\frac{\partial}{\partial y}\frac{\partial}{\partial y'}\int d\hat{\rho}\, e^{-(\vec{y}+\vec{y}')\cdot\hat{\rho}}$$

$$= -4\pi\frac{\partial}{\partial y}\frac{\partial}{\partial y'} j_0(|\vec{y}+\vec{y}'|) , \tag{A6}$$

where j_0 is the spherical Bessel function of order zero. We can decouple the $\vec{q}$ and $\vec{q}'$ integrations by employing an addition theorem for spherical Bessel functions[15] to write

$$K_{44}(\vec{q}+\vec{q}') = -(4\pi)^2\sum_{s=0}^{\infty}(-1)^s \frac{\partial j_s(y')}{\partial y'}\frac{\partial j_s(y)}{\partial y} \times \sum_{m_s=-s}^{s} Y_s^{m_s *}(\theta_q,\psi_q)Y_s^{m_s}(\theta_{q'},\psi_{q'}) , \tag{A7}$$

where j_s is the spherical Bessel function of order s and $Y_s^{m_s}$ the spherical harmonic of order s, m_s. Consequently we can write

$$\kappa_{4444}(\vec{q}+\vec{q}') = \frac{i}{2\pi}(n^2\tau_E)^{-1}(4\pi)^2\sum_{s=0}^{\infty}(-1)^s\frac{\partial j_s(y')}{\partial y'}\frac{\partial j_s(y)}{\partial y}\frac{4\pi}{3}\sum_{m_s=-s}^{s}\int_0^{2\pi}d\psi_q\int_0^{\pi}d\theta_q\sin\theta_q Y_1^0(\theta_q,\psi_q)Y_s^{m_s*}(\theta_q,\psi_q)$$
$$\times\int_0^{2\pi}d\psi_{q'}\int_0^{\pi}d\theta_{q'}\sin\theta_{q'}Y_s^{m_s}(\theta_{q'},\psi_{q'})Y_1^{0*}(\theta_{q'},\psi_{q'})$$
$$= \frac{i}{2\pi}(n^2\tau_E)^{-1}(4\pi)^2\sum_{s=0}^{\infty}(-1)^s\frac{\partial j_s(y')}{\partial y'}\frac{\partial j_s(y)}{\partial y}\frac{4\pi}{3}\sum_{m_s=-s}^{s}\delta_{m_s,0}\delta_{s,1}$$
$$= -\frac{i}{2\pi}(n^2\tau_E)^{-1}(4\pi^2)\frac{\partial j_1(y')}{\partial y'}\frac{\partial j_1(y)}{\partial y}\frac{4\pi}{3}\,. \tag{A8}$$

Note that the infinite sum over spherical Bessel functions of increasing order, when the angular wave-vector integrations are performed, collapses to just the $s=1$ term as it did for the transverse current contribution. Using the definition of $B_{44}(q)$ given in Table I and the definition of λ_E given in Eq. (2.3), one can write

$$\kappa_{4444}(\vec{q}+\vec{q}') = (\tfrac{4}{3}\pi)^2 B_{44}(q)(-i\lambda_E)^{-1}B_{44}(q')\,. \tag{A9}$$

In an analogous fashion, one can show that for the general term one has

$$\kappa_{KJI'K'}(\vec{q}+\vec{q}') = (\tfrac{4}{3}\pi)^2 B_{KJ}(q)(-i\lambda_E)^{-1}B_{I'K'}(q')\,. \tag{A10}$$

Note that there is an inherent asymmetry in this term. The summation indices K and K' can take on the values 2, 3, and 4, while the summation indices J and I' can take on the values 1, 2, 3, and 4. However, when $I'=1$, $\kappa_{KJI'K'}=0$, which is not generally the case for $J=1$. This asymmetry is reflected in the coupling to the fluid density fluctuations.

Following the procedures outlined above, one can show that performing the angular integrations in a term containing $(n-1)$ T matrix elements leads to the results

$$\int d\hat{\Omega}_{q_1}\int d\hat{\Omega}_{q_2}\cdots\int d\hat{\Omega}_{q_n}\epsilon_{K_1}T_{J_1I_2}(\vec{q}_1+\vec{q}_2)T_{J_2I_3}(\vec{q}_2+\vec{q}_3)\cdots T_{J_{n-1}I_n}(\vec{q}_{n-1}-\vec{q}_n)\epsilon_{K_n}$$
$$= (\tfrac{4}{3}\pi)^n B_{K_1J_1}(q_1)(-i\lambda_E)^{-1}B_{I_2I_2}(q_2)B_{J_2J_2}(q_2)$$
$$\times(-i\lambda_E)^{-1}B_{I_3I_3}(q_3)\cdots B_{J_{n-1}J_{n-1}}(-i\lambda_E)^{-1}B_{I_nK_n}(q_n)\,. \tag{A11}$$

Note that once again there is an asymmetry with respect to the index J_1 and the indices $I_2, I_3, \ldots, I_n$. If any of the indices $I_2, I_3, \ldots, I_n$ are set equal to one, then the whole term vanishes; however, this is not the case for $J_1=1$. The asymmetry in the coupling to the fluid density fluctuations is manifest in each of the repeated-ring contributions in Eq. (2.8).

APPENDIX B

The $\Delta_{IJ}(q,z)$ defined in Eq. (2.11) describe the intermediate propagation of the test particle and bath particles between correlated collisions. Approximations for some of the $\Delta_{IJ}(q,t)$ have appeared in Furtado *et al.*[7] and some in Résibois,[8] but with several typographical errors and with notational differences from our work. Thus, at the risk of some redundancy, we present the expressions that we have used in our numerical determination of the hard-sphere diffusion coefficient.

The free-particle correlation functions are

$$C_{s_{0_{11}}}(q,t) = C_{0_{11}}(-q,t) = C_{0_{22}}(-q,t)$$
$$= e^{-(y\tilde{l}\tau)^2/2}\,,$$

and

$$C_{0_{44}}(-q,t) = [1-(y\tilde{l}\tau)^2]e^{-(y\tilde{l}\tau)^2/2}\,. \tag{B1}$$

In Eqs. (B1), the dimensionless wave vector is $y=q\sigma$, the dimensionless mean free path is $\tilde{l}=[4\sqrt{\pi}n\sigma^3 g(\sigma)]^{-1}$, and the dimensionless time is $\tau=t/\tau_E$.

Exact expressions for the Enskog correlation

functions $C_{s_{E_{11}}}(q,t)$ and $C_{E_{IJ}}(-q,t)$ are not available. One can employ the techniques of kinetic modeling[19] to evaluate these correlation functions numerically over a wide range of wave vectors. Instead, we follow Résibois[8] and Furtado *et al.*[7] to approximate these correlation functions via analytic interpolation formulas. In this scheme, the basic ingredients used to represent a correlation function $C(q,t)$ are its short-time form $C^{st}(q,t)$, and its generalized hydrodynamic (long-time) form $C^h(q,t)$. These forms are connected via the interpolation formula

$$C(q,t)=C^{st}(q,t)e^{-(\alpha\tau)^2}+C^h(q,t)[1-e^{-(\alpha\tau)^2}]. \tag{B2}$$

The parameter α in Eq. (B2) has been set equal to $\frac{1}{3}$ as it was in the work of Resibois and Furtado *et al.* It is hoped that by interpolating between the correct short- and long-time behaviors, an adequate approximation is made for the correlation function.

The short-time behavior of the correlation functions is determined by a sum-rule analysis. Following Furtado *et al.* these short-time forms of the correlation functions of interest are

$$C^{st}_{s_{E_{11}}}(q,t)=\exp[-\tfrac{1}{2}(y\tilde{l}\tau)^2],$$

$$C^{st}_{E_{11}}(-q,t)=S(y)\exp[-(y\tilde{l}\tau)^2/2S(y)],$$

$$C^{st}_{E_{22}}(-q,t)=\exp\left\{-(y\tilde{l})^2\left[\frac{\tau f_1}{15\tilde{l}^2}+\frac{\tau^2}{2}\left(1+\frac{\sqrt{\pi}f_2}{15\tilde{l}}\right)^2\right]\right\},$$

and

$$C^{st}_{E_{44}}(-q,t)=[1-(y\tilde{l}\tau)^2X(y)]\times\exp\left[-(y\tilde{l})^2\left(\frac{\tau f_3}{5\tilde{l}^2}+\frac{\tau^2X(y)}{2}\right)\right]. \tag{B3}$$

The y-dependent functions $S(y)$, $X(y)$, and $f_i(y)$ are defined below. The generalized hydrodynamic forms of the correlation functions have also been determined by Furtado *et al.* They are

$$C^h_{s_{E_{11}}}(q,t)=\exp[-(y\tilde{l})^2\tilde{D}_E\tau],$$

$$C^h_{E_{11}}(-q,t)=S(y)\left[\frac{1}{\gamma(y)}\cos[c_s(y)y\tilde{l}\tau]\times\exp[-(y\tilde{l})^2\tilde{\Gamma}_E(y)\tau]+\left(1-\frac{1}{\gamma(y)}\right)\exp\left(-\frac{(y\tilde{l})^2\tilde{K}_E(y)}{C_p(y)}\right)\right],$$

$$C^h_{E_{22}}(-q,t)=\exp[-(y\tilde{l})^2\tilde{\nu}_E(y)\tau],$$

and

$$C^h_{E_{44}}(-q,t)=\cos[c_s(y)y\tilde{l}\tau]\exp[-(y\tilde{l})^2\tilde{\Gamma}_E(y)\tau]. \tag{B4}$$

In Eq. (B4), $\tilde{D}_E=\frac{3}{2}$ is the dimensionless self-diffusion coefficient; $S(y)$, $c_s(y)$, $\tilde{\Gamma}_E(y)$, $\tilde{K}_E(y)$, $C_p(y)$, and $\tilde{\nu}_E(y)$ are the dimensionless y-dependent static structure factor, adiabatic sound speed, coefficient of sound attenuation, thermal conductivity, specific heat at constant pressure, and kinematic viscosity, respectively; and $\gamma(y)=\frac{2}{3}C_p(y)$. The y-dependent quantities introduced above are

$$X(y)=\tfrac{1}{3}c_s^2(y)+\frac{4}{9}\left(1+\frac{2\sqrt{\pi}}{15\tilde{l}}f_5\right),$$

$$\tilde{\nu}_E(y)=\frac{5}{4}\left(1+\frac{\sqrt{\pi}f_2}{15\tilde{l}}\right)^2+\frac{f_1}{15\tilde{l}^2},$$

$$\tilde{\Gamma}_E(y)=\frac{5}{6}\left(1+\frac{\sqrt{\pi}f_2}{15\tilde{l}}\right)^2+\frac{f_3}{10\tilde{l}^2}+\frac{5}{36}\left(\frac{\sqrt{\pi}f_2}{15\tilde{l}}\right)^2-\frac{y^2f_3^2}{9800\tilde{l}}+\frac{\tilde{K}_E(y)}{2}\left(\frac{2}{3}-\frac{1}{C_p(y)}\right),$$

$$c_s^2(y)=[1-nC(y)]\gamma(y),$$

$$C_p(y)=\frac{3}{2}+\frac{(1+\sqrt{\pi}f_0/6\tilde{l})^2}{1-nC(y)},$$

and

$$\tilde{K}_E(y)=\frac{75}{16}\left(1+\frac{\sqrt{\pi}f_0}{10\tilde{l}}\right)^2+\frac{f_4}{6\tilde{l}^2}. \tag{B5}$$

In Eq. (B5), $C(y)$ is the hard-sphere direct correlation function. In our numerical analysis we used its Percus-Yevick form.[21] The $f_i(y)$ functions are

$$f_0(y)=\frac{3}{y^3}(\sin y-y\cos y),$$

$$f_1(y)=\frac{30}{y^5}(y\cos y-\sin y)+\frac{10}{y^2},$$

$$f_2(y)=\frac{15}{y^5}(3\sin y-3y\cos y-y^2\sin y),$$

$$f_3(y)=\frac{10}{3y^2}-\frac{10}{y^5}[(y^2-2)\sin y+2y\cos y], \tag{B6}$$

$$f_4(y)=\frac{6}{y^3}(y-\sin y),$$

$$f_5(y)=\frac{15}{2y^5}[(4y^2-9)\sin y+(9y-y^3)\cos y]$$

Note that these functions are all defined such that

$\lim_{y\to 0} f_i(y) = 1$.

Equations (B2)–(B6) completely specify the correlation functions $C_{s_{E_{11}}}$, $C_{E_{11}}$, $C_{E_{22}}$, and $C_{E_{44}}$ used in the numerical determination of the self-diffusion coefficient for a hard-sphere fluid.

The only quantities that remain to be specified are the nonconserved variable relaxation frequencies λ_s and λ for the test-particle and fluid fluctuations, respectively. In the spirit of the quasihydrodynamic approximation, λ_s and λ are to be set equal to the smallest nonconserved variable single-particle and fluid relaxation frequencies, respectively. For single-particle motion, the appropriate relaxation frequency is the smallest nonconserved variable matrix element of the test-particle Enskog memory function[22]

$$\lambda_s = \lambda_E = \tfrac{2}{3}\tau_E^{-1} = \bar{D}_E^{-1}\tau_E^{-1}. \tag{B7}$$

In an analogous fashion we can relate λ to the smallest nonconserved variable matrix element of the fluid Enskog memory function.[23] One finds that

$$\lambda = \tfrac{4}{5}\tau_E^{-1}. \tag{B8}$$

In analogy with Eq. (B7) one would expect that a better approximation to λ would be to relate it to the fluid kinematic viscosity as

$$\lambda = \tilde{\nu}_E^{-1}(y=0)\tau_E^{-1}. \tag{B9}$$

This is the value λ used to obtain Figs. 1 and 2.

In this Appendix we have specified the forms of the quantities appearing in Eq. (2.11) for $\Delta_{IJ}(q,z)$. Substituting these expressions into Eq. (2.11) we find that the Laplace transform can be computed analytically. The resultant expressions for Δ_{IJ} are substituted into Eq. (2.14), and the q integration performed numerically to determine $R_\perp^1$, $R_\parallel^1$, and R_n^1. Substituting these results into Eq. (2.20) we obtain D/D_E.

[1]B. J. Alder, D. M. Gass, and T. E. Wainwright, J. Chem. Phys. 53, 3813 (1970).

[2]J. R. Mehaffey and R. I. Cukier, Phys. Rev. Lett. 38, 1039 (1977).

[3]J. R. Mehaffey and R. I. Cukier, Phys. Rev. A 17, 1181 (1978).

[4]G. F. Mazenko, Phys. Rev. A 7, 209 (1973); 7, 222 (1973); 9, 360 (1974).

[5]Repeated rings were introduced in M. H. Ernst and J. R. Dorfman, Physica (Utr.) 61, 157 (1972); J. R. Dorfman, H. van Beijeren, and C. F. McClure, Arch. Mech. Stosow. 28, 333 (1976).

[6]B. J. Alder, W. E. Alley, and J. H. Dymond, J. Chem. Phys. 61, 1415 (1974); A. Rahman, J. Chem. Phys. 45, 2585 (1966).

[7]P. M. Furtado, G. F. Mazenko, and S. Yip, Phys. Rev. A 14, 869 (1976).

[8]P. Résibois, J. Stat. Phys. 13, 393 (1975).

[9]S. Chapman and T. G. Cowling, *The Mathematical Theory of Nonuniform Gases*, 3rd ed. (Cambridge University, Cambridge, 1970), Chap. 16.

[10]H. H. U. Konijnendijk and J. M. J. van Leeuwen, Physica (Utr.) 64, 342 (1975).

[11]It should be noted that we have neglected here the contribution in $R(z)$ coming from processes in which the intermediate propagation between correlated collisions involves the test-particle free streaming and its collision partner experiencing only the mean-field interaction (direct correlation function) of the fluid. Such contributions are expected to be small.

[12]The $\vec{q}$ reference frame is defined to have its z axis along $\vec{q}$ and to be related to the laboratory reference frame via the Euler angles θ_q, ϕ_q, and ψ_q.

[13]H. Goldstein, *Classical Mechanics* (Addison-Wesley, Cambridge, Mass., 1950), p. 107.

[14]J. R. Mehaffey and R. C. Desai, J. Chem. Phys. 66, 4721 (1977).

[15]C. J. Tranter, *Bessel Functions with Some Physical Applications* (Hart, New York, 1968), p. 37f.

[16]As was pointed out in Appendix A, in the derivation of Eq. (2.13) we have ignored the coupling to the fluid energy (temperature) fluctuations (i.e., the momentum state $|5\rangle$). Such contributions are expected to be smaller than those arising from the coupling to the fluid density and current fluctuations. Further, in going from Eq. (2.13) to Eq. (2.15) we have ignored contributions from the fluid density-longitudinal current cross terms $\Delta_{14} = \Delta_{41}$. Such contributions can be retained in the theory and the resultant expressions can be summed. If one follows Eq. (2.14) to define the single-ring cross term $R^1_{n,\parallel}(z)$ in terms of Δ_{14}, one finds the sum of the Enskog and repeated-ring memory functions is $\Lambda + R = -i\lambda_E\{\{1 - [(R_n^1 + R^1_{n,\parallel})/i\lambda_E] + \frac{1}{2}(R^1_{n,\parallel}/i\lambda_E)[(R_\perp^1 + R_\parallel^1 + R_n^1 + R^1_{n,\parallel})/i\lambda_E]\}\}\{1 + [(R_\perp^1 + R_\parallel^1)/i\lambda_E]\}^{-1}$. This should be compared with Eq. (2.16). We have numerically evaluated $R^1_{n,\parallel}$ employing the techniques outlined in Sec. III and Appendix B, and found it to be small relative to R_n^1, $R_\perp^1$, and $R_\parallel^1$. Consequently we have explicitly ignored $R^1_{n,\parallel}$ in our presentation.

[17]B. J. Alder and T. E. Wainwright, Phys. Rev. A 1, 18 (1970); E. H. Hague and A. Martin-Lof, J. Stat. Phys. 7, 259 (1973); R. Kapral and M. Weinberg, Phys. Rev. A 8, 1008 (1973); 9, 1676 (1974); Y. Pomeau and P. Résibois, Phys. Rep. C 19, 63 (1975).

[18]K. Kawasaki and I. Oppenheim, Phys. Rev. 136, A1519 (1964); J. R. Dorfman and E. G. D. Cohen, Phys. Rev. Lett. 25, 1257 (1970); Phys. Rev. A 6, 776 (1972); 12, 292 (1975); J. Dufty, *ibid.* 5, 2247 (1972); G. F. Mazenko and S. Yip, in *Modern Theoretical Chemistry*, edited by B. J. Berne (Plenum, New York, 1977); P. Résibois and J. L. Lebowitz, J. Stat. Phys. 12, 483 (1975); I. deSchepper, Ph.D. thesis (Catholic

University of Nijmegen, 1974) (unpublished); P. Résibois, J. Stat. Phys. 13, 393 (1975).
[19]G. F. Mezenko, T. Y. C. Wei, and S. Yip, Phys. Rev. A 6, 1981 (1972); A. Sugawara and S. Yip, Phys. Fluids 11, 925 (1968).
[20]P. T. Herman and B. J. Alder, J. Chem. Phys. 56, 987 (1972); K. Toukubo, K. Nakanishi, and N. Watanabe, *ibid.* 67, 4162 (1977).
[21]N. W. Ashcroft and J. Lekner, Phys. Rev. 145, 83 (1966).
[22]Here we mean the Enskog memory function $\phi_{s_E}^{\alpha\alpha}(13)$ of the kinetic equation for the test-particle phase-space density correlation function [cf. Eq. (2.9) in Ref. 3]. The matrix elements of $\phi_{s_E}^{\alpha\alpha}$ are defined by Eq. (3.6b) of Ref. 3.
[23]Some of these matrix elements are presented in P. M. Furtado, G. F. Mazenko, and S. Yip, Phys. Rev. A 13, 1641 (1976). We only use their small-wave-vector limit.